Macroinitiator and Macromonomer Modified Montmorillonite for the Synthesis of Acrylic/MMT Nanocomposite Latexes

Gabriela Diaconu, Matej Mičušík, Audrey Bonnefond, Maria Paulis, and Jose R. Leiza*

Institute for Polymer Materials, POLYMAT and Grupo de Ingeniería Química, Dpto. de Química Aplicada, University of the Basque Country, Joxe Mari Korta zentroa, Tolosa Etorbidea 72, 20018 Donostia-San Sebastián, Spain

Received November 4, 2008; Revised Manuscript Received March 17, 2009

ABSTRACT: A cationic macromonomer, 2-methacryloylethylhexadecyldimethylammonium bromide MA16, and a cationic macroinitiator, cationic acrylic/styrene oligomer end-capped with a nitroxide, were used to modify pristine Na−MMT, to enhance compatibility between the clay platelets and the host acrylic polymer matrix in waterborne nanocomposites. Both cationic species were successfully exchanged in the montmorillonite. The organically modified clays were used for the synthesis of acrylic (MMA/BA)/clay waterborne nanocomposites by miniemulsion polymerization. The 30% solids containing latexes were stable and coagulum free and presented better mechanical, thermal and barrier properties than the pristine acrylic copolymer.

Introduction

Polymer matrix based nanocomposites have become a prominent area of current research and development. Waterborne polymer/clay nanocomposites comprise organic/inorganic hybrid particles containing polymer matrices and platelet-shaped clay particles. Layered silicate clays such as montmorillonite (MMT) consist of stacks of platelets, with each platelet having a thickness of ∼1 nm and a mean aspect ratio of ∼166.[1] The interlayer distance in the clay galleries is around 11.5 Å. Exfoliated clay-based nanocomposites have dominated the hybrid polymer literature.[2] Anyway the exfoliation of the clay to the level of individual platelets throughout the polymer matrix is still a big challenge. Polymer/clay nanocomposites exhibit improved properties when compared to the pure polymer, such as enhanced mechanical and thermal properties, reduced gas permeability, high fire resistance and lower flammability.[3−5] The first successful polymer/clay nanocomposites can be traced back in 1993 through the effort of the Toyota's group when they obtained exfoliated Nylon-6/clay via *in situ* polymerization of ε-caprolactam.[6] Since then a large variety of polymers[7−12] have been used to obtain polymer/clay nanocomposites while the most frequently clay used for this category of materials has been montmorillonite.

The *in situ* polymerization is the most common method used for the production of a wide variety of polymer/clay nanocomposites. In this method, the layered silicate is swollen within the liquid monomer or a monomer solution, so that polymer formation can occur between the intercalated sheets. This strategy requires a pretreatment of the clay in order to improve its compatibility with the host monomer/polymer and achieve a good dispersion. This can be achieved by replacing the interlayer cations by suitable organic compounds. These organic cations can act just as organic compatibilizers,[13−18] or they can bear on one end a functional reactive group (monomer or initiator molecule) that can participate in the polymerization process and promote exfoliation of the clay layers.[15,19−22] Reactive monomer groups were introduced by Akelah and Moet,[23] who modified the Na− and Ca−montmorillonite with (vinylbenzyl)trimethyl ammonium chloride, increasing the interlayer space by 5.4 Å. These modified clays were used for the preparation of intercalated polystyrene/clay nanocomposites with interlayer spacing between 17.2 and 24.5 Å depending on the nature of the solvent used for *in situ* solution polymerization. Surface initiated polymerization was also performed from clay surface by exchanging cationic initiators in the clay galleries.[24−26] In order to regulate polymer chain growth within the interstitial spaces controlled or living polymerization techniques bring outcome. Weimer et al.[25] demonstrated that polystyrene (PS) chains could be grown from the surface of the montmorillonite by a nitroxide-mediated polymerization (NMP) technique using a silicate-anchored alkoxyamine initiator of the 2,2,6,6-tetramethylpiperidine *N*-oxide (TEMPO) derivative. Bourgeat-Lami et al.[27] used the same technique to grow PS chains from Laponite platelets. For the functionalization of the Laponite platelets, they used an alkoxyamine initiator based on *N*-*tert*-butyl-*N*-[1-diethylphosphono-(2,2-dimethylpropyl)], DEPN, carrying a terminal quaternary ammonium functional group for electrostatic anchoring to the clay layers. Zhang et al.[28] used the *in situ* RAFT polymerization[29] with a RAFT agent-intercalated MMT (10-carboxylic acid-10-dithiobenzoatedecyltrimethylammonium bromide (CDDA) modified Na−MMT clay) to produce polystyrene/MMT nanocomposites with exfoliated structure and higher thermal stability compared to pure PS. All these works used solution or bulk polymerization techniques.

The scope of this work was to prepare waterborne polymer/clay nanocomposites for coating applications, starting from organically modified montmorillonites bearing a reactive group. Emulsion polymerization has been the polymerization technique most extensively used for the production of waterborne polymer−clay nanocomposites, due to the complete dispersion (exfoliation) of sodium montmorillonite (Na−MMT) in water.[30−35] However the use of organically modified clays does not allow their direct use in emulsion polymerization, as they are not dispersed in water. In some cases clay aggregation (when dispersed in water) was avoided by a post-treatment, as it was shown by Negrete-Herrera et al.[36,37] for laponite modified with AIBA (2,2-azobis(2-methylpropionamidine) hydrochloride). In other processes, the modified clays were dissolved in the monomer, which was polymerized by a conventional emulsion polymerization procedure.[38−41] In this case, the organophilic clay cannot be incorporated into the polymer particles because diffusion through the water phase is not favored.

In order to overcome diffusion limitations given by the phase transfer events in conventional emulsion polymerization a

* To whom correspondence should be addressed: E-mail: jrleiza@ehu.es. Telephone: (+34) 943015329. Fax: (+34) 943017065.

10.1021/ma802467j CCC: $40.75
Published on Web 04/13/2009

promising approach for synthesizing waterborne polymer/clay nanocomposite particles (in the submicrometer range) using organically modified clays is miniemulsion polymerization.[42,43] In this polymerization the monomer droplets might contain the hydrophobic clay stacks that upon polymerization (ideally the nucleation and polymerization occurs in the miniemulsion droplets) might lead to exfoliated nanostructures. There are very few examples in the literature where miniemulsion polymerization has been used to prepare waterborne polymer/clay nanocomposites.[44−47] All of them presented styrene polymerizations (or copolymerization with acrylics[46]), in the presence of modified laponite,[44] saponite,[45] or montmorillonite.[46,47] The solids contents of the reported stable latexes ranged from 5 to 20%, needing high amounts of emulsifier to stabilize the latexes (in some cases up to 17%[45]), which is a drawback for application properties in adhesives and coatings. We have recently shown that all acrylics (methyl methacrylate/butyl acrylate, MMA/BA: 50/50 wt %) stable and coagulum free latexes with solids contents up to 42% with Cloisite 30B (commercial organically modified clay) can be obtained by miniemulsion polymerization with 4% of sodium lauryl sulfate as emulsifier.[48]

The goal of this work was to improve the compatibility of the clay platelets with the polymer matrix (MMA/BA: 50/50 wt %) by using an organically modified clay bearing a reactive group, as just surface location of the Cloisite 30B was found in previous works.[48] Two kinds of organic modifiers were used: a cationic macromonomer, 2-methacryloylethylhexadecyldimethylammonium bromide (MA16) and a cationic macroinitiator, acrylic oligomer end-capped with a nitroxide. MA16 has a cationic site for cationic exchange with the clay, a long alkyl chain that will compatibilize with the polymer matrix and a reactive group, a methacrylate double bond, that can covalently bond the clay platelets to the polymer matrix by polymerization in the interlayer space. The cationic macroinitiator is a living oligomer composed by a cationic quaternary ammonium group for the cationic exchange with the interlayer cations, a hydrophobic chain compatible with the polymer matrix (MMA/BA) made of MMA and S units, and a reactive group produced by using a nitroxide agent during the synthesis.

The article is organized as follows: first, the experimental procedure, including the synthesis and cationic exchange of the organic modifiers in Na−MMT, and characterization techniques are described in detail. Second, polymerization kinetics and latex properties are presented and discussed. Finally the morphological properties of the nanocomposite films are discussed, and mechanical, thermal and permeation properties of the waterborne nanocomposite films are presented and compared with pristine copolymer latex prepared under the same conditions.

Experimental Section

Materials. Commercial natural clay, CloisiteNa, was provided by Southern Clay Products Inc. (Texas/USA). It has a cationic exchange capacity of 92.6 mequiv/100 g of clay and its XRD analysis shows that the interlayer space is 1.15 nm. Methyl methacrylate, MMA, butyl acrylate, BA, and styrene, S (Quimidroga), were used as monomers. Sodium lauryl sulfate (SLS, Aldrich) was used as emulsifier. Stearyl acrylate (SA, Aldrich) was used as costabilizer. AIBA (2,2′-azobis(2-amidinopropane) dihydrochloride, WAKO), ascorbic acid (AsAc, Aldrich) and *tert*-butyl hydroxyperoxide (TBHP, Panreac) were used as initiators, and SG1 (*N*-*tert*-butyl-*N*-(1-diethylphosphono-2,2-dimethylpropyl) nitroxide, kindly supplied by ARKEMA) as control agent. 1-Bromohexadecane (Aldrich) and 2-(dimethylamino) ethyl methacrylate (Aldrich) were used for the synthesis of MA16. All materials were used as received.

Preparation of Organically Modified Clays. *1. Cationic Macromonomer (MA16) Preparation and Intercalation.* MA16 was synthesized according to the synthetic procedure used by Zeng et al.[49] as follows: 1-bromohexadecane and 2-(dimethylamino) ethyl methacrylate (1:2 molar ratio) were reacted at room temperature for 24 h in presence of the inhibitor hydroquinone monomethyl ether (see Scheme 1). The resulting precipitate of MA16 was purified by filtering and washing using ethyl acetate. The white powder was dried under vacuum at room temperature for 24 h and then analyzed by ^{1}H NMR analysis (see Supporting Information), which evidenced resonance signals for all the protons of the MA16 molecule, confirming the successful synthesis of the MA16.

Scheme 1. Synthesis of the MA16 Cationic Macromonomer[49]

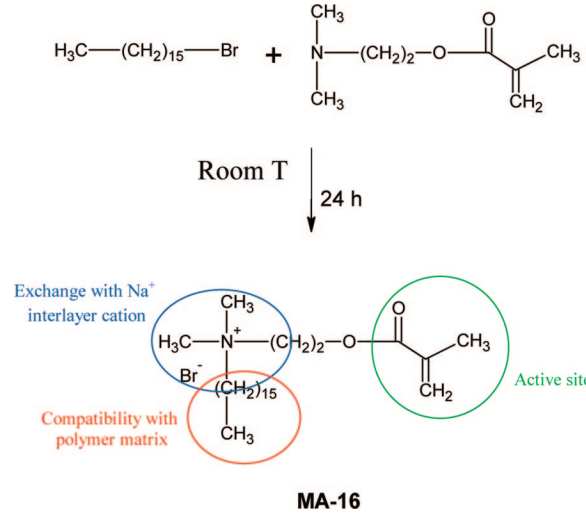

The organic modification of the Na−MMT clay with MA16 was carried out as follows:[50] 2 g of Na−MMT clay were dispersed in 80 mL distilled water by stirring overnight at room temperature. An excess of MA16 (2 mequiv/g of clay) was dissolved in 20 mL of distilled water, and then continuously added dropwise to the clay dispersion that was stirred at 3 °C. The cationic exchange was carried out at 3 °C for three hours. Afterward, the MA16-MMT clay was filtrated and washed several times with distilled water in order to wash off the possible adsorbed MA16, and then dried in a vacuum oven at room temperature for 24 h.

To evaluate the organic part of organomodified clays, the values of residue and weight loss from calcination was used. The calcination was performed in the oven at 500 °C for 12 h. The calculation was done according to the following equation:

$$\frac{\left(\text{weight } loss - \frac{7}{93}\times\text{residue}\right)/M_w}{\left(\text{residue} + \frac{7}{93}\times\text{residue}\right)} = \text{mequiv/g of clay} \quad (1)$$

taking into account the 7% of weight loss of CloisiteNa on ignition given by the producer. M_w is the molar mass of the modifier.

In the case of just filtrated MA16 modified clay a residue of 60.6 wt % was obtained, which corresponds to 1.40 mequiv of MA16 exchanged per g of clay.

2. Cationic Macroinitiator Preparation and Intercalation. The living oligomer with a cationic group was synthesized in aqueous phase by polymerizing methyl methacrylate and styrene (below their water solubility: MMA = 1.5×10^{-1} mol/L, $S = 4.3 \times 10^{-3}$ mol/L) using AIBA (2,2′-azo-bis(2-amidinopropane) dihydrochloride) as initiator, and in presence of a nitroxide, SG1 (*N*-*tert*-butyl-*N*-(1-diethylphosphono-2,2-dimethylpropyl) nitroxide). The polymerization reaction was carried out in a 2 L stirred tank reactor. The procedure used for the preparation of oligomers with 20 monomer units was as follows: the mixture of monomers (MMA, 3.86×10^{-2} mol; S, 4.3×10^{-3} mol), water (1900 mL) and SG1 (2.36×10^{-3} mol) was charged in the reactor and then deoxygenated by purging with a gentle flow of nitrogen (15 mL/min) for 15 min at room temperature. Afterward, the temperature was raised to 90 °C under nitrogen flow (15 mL/min) and an aqueous solution of AIBA

Scheme 2. Chemical Structure of the Cationic Macroinitiator Used To Modify Na−MMT

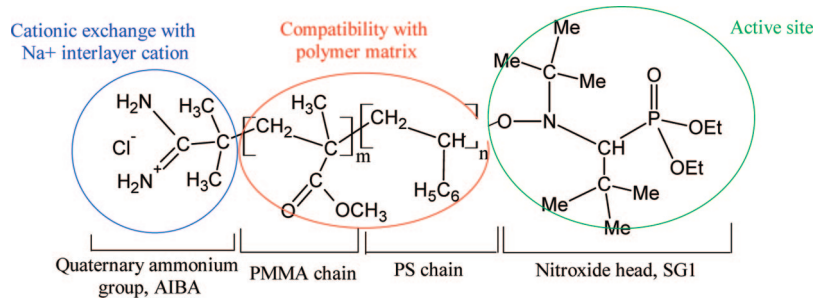

Table 1. Formulation Used To Prepare the Miniemulsions

component	amount (g)	parts per hundred monomers (Pphm)
	Oil Phase	
MMA	135	50
BA	135	50
SA	8.1	3
clay	8.1−30	1.8−4
	Aqueous Phase	
SLS	10.8	4
deionized water	480	177.7

(2.15×10^{-3} mol) was added to the reactor. The reactor content was allowed to polymerize for 24 h at 90 °C. To ensure the livingness of the chains comonomer molar ratio MMA/S was 90/10 mol % according to Charleux et al.[51] The molar ratio SG1:AIBA was 1.1.

Scheme 2 shows the chemical structure of the cationic macroinitiator that contains a cationic site, the MMA/S oligomer, and the active site, the end-capped nitroxide group.

The conversion was measured by gravimetric analysis to be 67.4%. The ^{1}H NMR analysis (see Supporting Information) of the cationic oligomer presented peaks corresponding to the methylene ($-CH_2-$) and methoxy ($-OCH_3$) protons of MMA at 2.17 ppm and 3.6 ppm, respectively; the C−H protons and phenyl protons of styrene at 2.49 ppm and 7.0−7.5 ppm range; and the $-NH_2$ and $-O-CH_2-$ protons at 1.26 and 4.24 ppm (indicating the existence of the amine and nitroxide groups in the MMA/S oligomer chain). The presence of all these peaks confirmed that the MMA/S based cationic macroinitiator containing one amine group in one end, and one end-capped living radical in the other end was successfully synthesized. From the ^{1}H NMR spectrum the composition of the cationic oligomer was calculated to be MMA/S = 88/12 mol%, which was close to the monomer loaded to the reactor. The molecular weight distribution of the synthesized cationic oligomer was measured by SEC. A narrow molecular weight distribution (P.I. = 1.1) was obtained with a number average molecular weight of 1170 g/mol, which corresponds to an oligomer with an average number of 8 monomer units.

The cationic exchange of the Na−montmorillonite with this cationic oligomer was as follows: to the cationic oligomer aqueous dispersion (4.2 g of cationic oligomer) an aqueous solution of Na−MMT (3 g Na−MMT in 200 mL of H_2O) was added; and the mixture was stirred for 3 h. The resultant precipitate was collected and washed several times with distilled water in order to get rid of the possible adsorbed oligomer. The organically modified MMT clay was dried at 60 °C for 24 h. The extent of the cationic exchange was determined from the residues obtained by calcination. In the case of the cationic macroinitiator−MMT, the residue was 36.34 wt % and hence the cationically exchanged macroinitiator was 1.33 mequiv/g of clay (for an average molecular weight of 1170 g/mol).

Miniemulsion Preparation. The miniemulsions were prepared using the recipe presented in Table 1 as follows: the oil phase was prepared by dissolving the costabilizer (stearyl acrylate, 8.1 g) and the organically modified clay (8.1−30 g) in the monomers (MMA and BA; 50/50 wt %, 270 g). This mixture was stirred for 15 min at 1000 rpm with a magnetic stirrer. The aqueous phase was prepared by dissolving the emulsifier (sodium lauryl sulfate, 10.8 g) in water (480 g). Both phases (aqueous and oil phase) were brought together and mixed for 15 min at 1000 rpm. The dispersion was sonified using a Branson Sonifier 450 (operating at 8-output control and 80% duty cycle for 15 min in an ice bath and under magnetic stirring). In order to avoid coagulation between clay layers,[52] the miniemulsion was carried out at basic pH (pH = 9), which was achieved by adding boric acid into the oil phase and adjusting the pH with NH_4OH. A blank miniemulsion (without clay) was prepared in the same way.

Miniemulsion Polymerization. All of the reactions were carried out in a 1000 mL glass jacketed reactor fitted with a reflux condenser, sampling device, N_2 inlet, two feeding inlets and a stainless steel anchor stirrer equipped with two blade impellers rotating at 250 rpm. Reactor temperature and initiator feed flow rates were controlled by an automatic control system (Camile TG, Biotage). The latexes, with solids content of 30wt % were synthesized batchwise. The miniemulsion prepared as above was charged in the reactor and the temperature raised to 70 °C or to 90 °C (in the case of the cationic macroinitiator formulation) under gentle nitrogen flow. Upon reaching the reaction temperature, aqueous solutions of the redox components (TBHP/AsAc = 2:1 mol ratio) were fed to the reactor in two separate streams (0.675 and 1.25 g in 75 g of water each, respectively) for 2 h. In the case of the macroinitiator exchanged montmorillonite, the reaction was kept at 90 °C for 4 h without further initiator addition, and after the redox initiator system was fed to the reactor for 2 h.

Characterization and Measurements. Polymer particle and monomer droplet sizes were measured by dynamic light scattering using a Coulter N4 Plus in unimodal analysis. For this analysis, a fraction of the latex (or miniemulsion) was diluted with deionized water (saturated with monomers in the case of miniemulsion droplet size measurement). The reported particle size (droplet size) values represent an average of three repeated measurements. Conversion was measured by gravimetry.

Wide-angle X-ray diffraction (WAXD) analyses were performed on a Philips PW 1729 Generator connected to a PW 1820 (Cu Kα radiation with $\lambda = 0.154056$ nm) at room temperature. The range of the diffraction angles was $2\theta = 2-12°$ with a scanning rate of 0.02°/3 s. The (001) basal spacing of the clay (d) was calculated using the Bragg equation: $n\lambda = 2d(\sin\theta)$. To perform the WAXD analysis, the films cast from the latex were thoroughly rinsed to get rid of the SLS and to avoid its peaks at 7, 5, and 2.5° in the WAXD patterns.

Small-angle X-ray scattering (SAXS) measurements were carried at the Spanish CRG beamline BM16 in the European Synchrotron Radiation Facility in Grenoble, France. The monochromatic X-ray beam wavelength was λ=0.978 nm with a sample-to-detector distance of 3.93m. A 2-D detector marCCD165 was used and the obtained two-dimensional scattering patterns were radially averaged using FIT2D program to obtain the scattered intensity ($I(q)$) profiles as a function of the scattering vector (q). The samples were calibrated to the diffraction peaks of silver−behenate.

The morphology of the nanocomposite films was studied by means of a transmission electron microscope, TEM, (Hitachi 7000FA at 75 kV). Two different samples were analyzed by TEM,

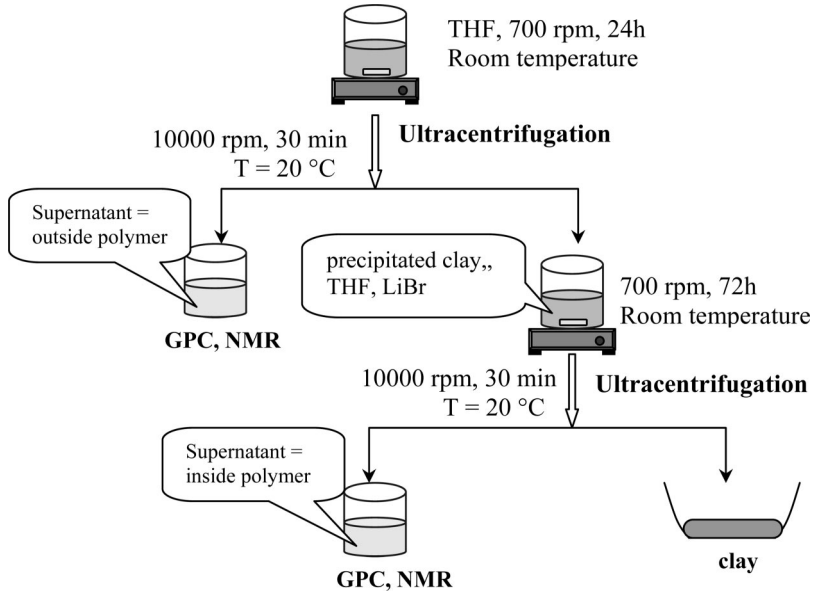

Figure 1. Schematic representation of the reverse cationic exchange procedure used to recover the polymer attached to the clay.

namely the dried films and the dried diluted latexes. The dried films were cryosectioned with a LEICA ULTRACUT FCS cryoultramicrotome using a DIATOME 35 degrees diamond knife. The ultrathin sections were placed on a 300 mesh Formvar coated copper grid and observed with the transmission electron microscope. The liquid samples were analyzed by negative staining. The typical procedure for preparation of the negatively stained specimens was as follows: a droplet of latex placed on a clean Parafilm surface was touched with a copper grid coated with Formvar and carbon for one minute. After cleaning the excess of latex (5 times with MiliQ water), the grid was immersed in 2% aqueous solution of negative stain (uranyl acetate) for 90 s. Then, the excess of stain was removed and the grid with the stained sample was allowed to air-dry at room temperature.

The molecular weight distribution, MWD, of the nanocomposite latexes was determined. First the amount of insoluble polymer was measured by conventional Soxhlet extraction[53] of the dried latex in THF under reflux conditions, and the soluble fraction was injected into a size exclusion chromatograph, SEC, to determine the distribution and the number and weight molecular weight averages. Apart from the analysis of the soluble polymer MWD, the study of the M_w of the polymer end-tethered to the clay was carried out. For the analysis of the inside copolymers, a reverse cationic exchange procedure was used. The typical polymer recovery process was as follows: 1 g of prepared nanocomposite film and 100 mL of THF were stirred at room temperature for 24 h. After 24 h of stirring, the solution was ultracentrifuged at 10 000 rpm, $T = 20$ °C for 30 min to separate the polymer formed outside the clay platelets from the clay. The supernatant was concentrated and further analyzed by GPC and NMR (outside polymer). The precipitated clay was dispersed in THF (25 mL) and 0.3 g of LiBr was added for the reverse cationic exchange. The mixture was mixed at room temperature at 700 rpm for 72 h. Afterward, the mixture was ultracentrifuged at 10 000 rpm, $T = 20$ °C for 30 min to separate the polymer formed inside the clay platelets from the clay. The supernatant was used for GPC and NMR analysis (inside polymer). The precipitated clay was dried at 60 °C for 24 h. Figure 1 shows a schematic representation of the polymer recovery process.

Dynamic mechanical thermal analysis (DMTA) was used to analyze the thermo-mechanical behavior of the polymer/clay nanocomposites. To perform the DMTA analysis a latex film 1 mm thick was heated from −50 to 100 °C with a heating rate of 0.3 °C/min. The thermal stability of the nanocomposites was studied by thermogravimetric analysis (TGA). To perform the TGA analysis the sample was heated from 20 to 600 °C with a heating rate of 10 °C/min using TA Instruments Thermogravimetric Analyzer model Q500.

Water vapor permeability tests were carried out to the nanocomposite films placing them in the upper part of a cell filled with water. The permeability was also measured to the films upon rinsing them with water. The water vapor transfer rate (WVTR, g mm/cm^2 days) was calculated with the following equation:[54]

$$\mathrm{WVTR} = 8.64 \times 10^5 \frac{Bt}{A(1 - a_{ext})} \tag{2}$$

where B is the slope of the water vapor loss (g/s), t is the thickness of the latex film (mm), A is the area of the latex film ($A = 2.54$ cm^2), and a_{ext} is vapor activity (measured using a thermohygrometer). The measurements were carried out in a temperature controlled chamber at 30 °C and the weight loss of the water vapor was recorded every 15 s for 4 h. Contact angle measurements were carried out in a OCA 2000 (DataPhysics) instrument on as prepared and rinsed films.

Results and Discussions

Cationic Exchange. The success of the cationic exchange was analyzed by WAXD, and the results are plotted in Figure 2.

It can be observed that the (001) diffraction peak of clay modified by the cationic macroinitiator appeared at smaller angles ($2\theta = 5.77°$) compared to the Na−MMT diffraction peak ($2\theta = 7.6°$), indicating that the cationic exchange took place successfully, and that the basal space increased from 1.15 nm for Na−MMT to 1.53 nm. The MA16-MMT clay presented two peaks, one at 2.69° (3.28 nm) and the second one at 4.65° (1.89 nm). This was not expected and the nature of the two peaks was further analyzed. Thus, the WAXD pattern of pure MA16, which is a crystalline solid, presented a peak at 2.9°. Therefore, the first peak of the MA16-MMT can be attributed to crystalline MA16. This result indicated that an ordered structure of MA16 molecules in the intergallery could have formed. To assess this assumption the modified clay was extracted in THF under reflux and analyzed again by WAXD upon drying. The XRD pattern of the extracted MA16-MMT showed only one peak at ca. 4.65°. Calcination of the as prepared and extracted MA16-MMT also confirmed the different amounts of MA16 molecules in the clay galleries. The as prepared MA16-MMT had a residue of 60.6 wt % and the

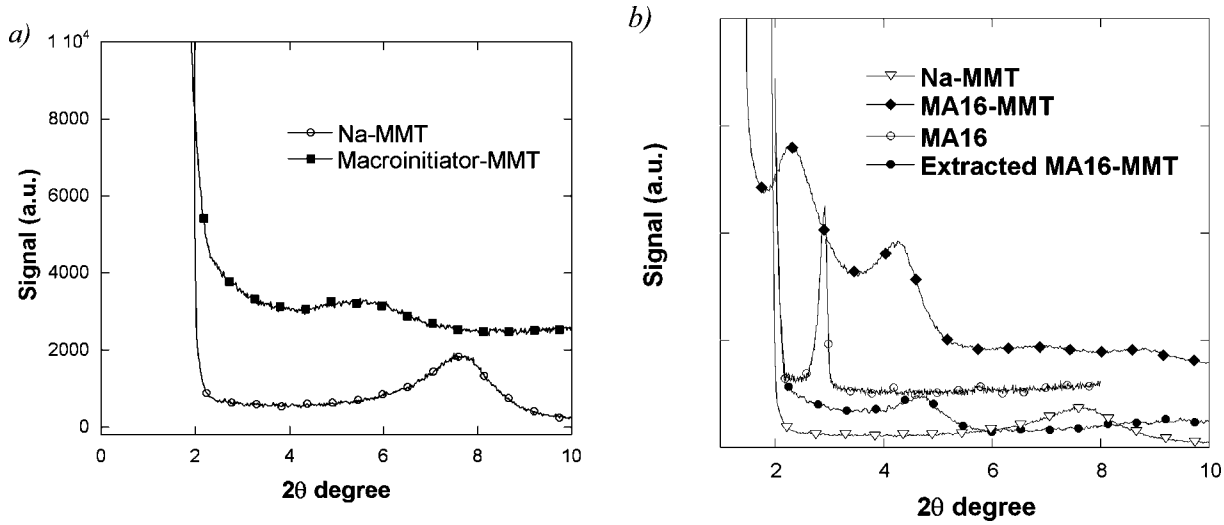

Figure 2. WAXD patterns of the Na−MMT and (a) macroinitiator-MMT and (b) MA16-MMT, extracted MA16-MMT, and pure MA16.

Table 2. Summary of the Nanocomposite Latexes with 30 wt % Solids Content Synthesized by Means of Batch Miniemulsion Polymerization with Reactive Montmorillonite Clays

run	type of clay	reactive clay percentage [a] (wt %)	theoretical MMT clay percentage [a] (wt %)
MP		0	0
MPCO	macroinitiator-MMT	11.1	4
MPCM	MA16-MMT	3	1.8

[a] Based on the total amount of the monomer in the recipe.

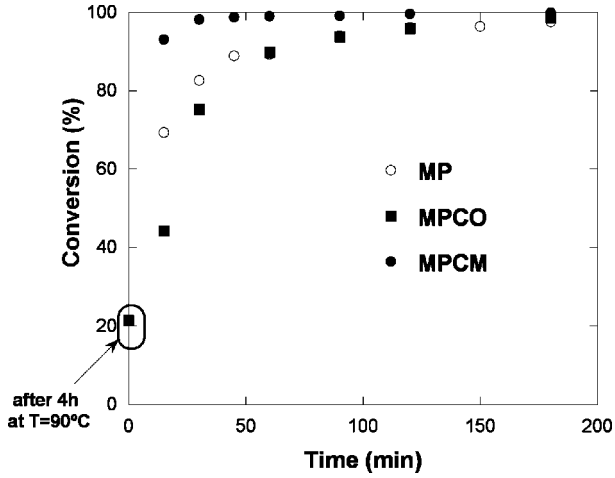

Figure 3. Time evolution of the conversion for the batch miniemulsion polymerization experiment carried out with and without reactive montmorillonite clays.

extracted one, 62.8 wt %. Since alkylammonium cations are adsorbed inside the interlayer through both cation exchange and hydrophobic bonding, using an excess of the organomodifier (above the CEC of the clay) creates a more packed and organized structure inside the clay galleries. A similar behavior during cationic exchange of Na−MMT was observed by Marras et al.,[55] who observed a formation of pseudotrimolecular layer, when the alkyl ammonium cation concentration reaches 200% of the clay CEC. In the following polymerization reactions only the filtrated MMT-MA16 with 1.89 nm interlayer space and some extra MA16 (1.40 mequiv/1 g of clay) inside the clay galleries was used.

Miniemulsion Polymerization Kinetics. Table 2 presents a summary of the experiments carried out with indication of the type and percentage of the clay used in each experiment.

Table 3. Monomer Miniemulsion Droplet Size and Final Particle Size of the Latexes Synthesized in the Presence of Reactive MMT Clays

run	type of clay	miniemulsion droplet size (nm)	final particle size (nm)
MP		108	93
MPCO	macroinitiator-MMT	220	136
MPCM	MA16-MMT	202	112

Table 4. Droplet Surface Area (A_D) and the Area Covered by the Emulsifier (A_E)[a]

Run	A_D (Å^2)	A_E (Å^2)	Free emulsifier (mM)	N_p/N_d
MP	1.66×10^{24}	2.94×10^{24}	27.3	1.6
MPCO	2.0×10^{23}	7.23×10^{23}	48.3	4.2
MPCM	2.17×10^{23}	7.23×10^{23}	44.7	5.9

[a] A_D is the surface area formed by the droplets; $A_E = (\text{c-cmc})a_S N_A V$ is the surface area that could be covered by emulsifier. Free emulsifier = (c-cmc) − $A_D/a_S N_A V$. N_d is the droplets number; N_p is the polymer particles number.

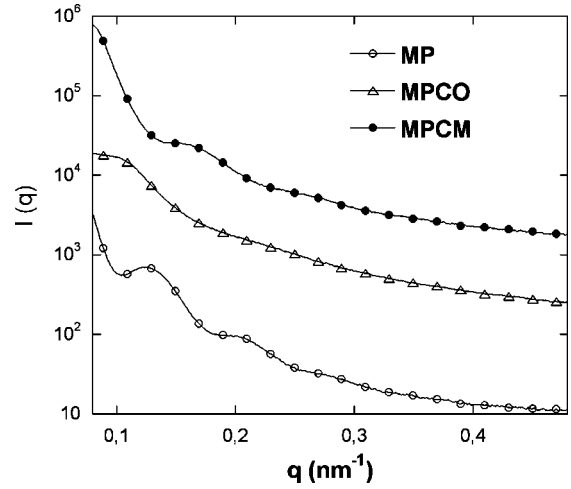

Figure 4. SAXS patterns of blank latex MP and nanocomposite latexes MPCO and MPCM.

Figure 3 presents the time evolution of conversion for the blank run MP and the runs with the modified montmorillonites, MPCO and MPCM. It can be observed that the miniemulsion polymerization reactions were fast and full conversion was reached in 60−90 min. The polymerization process for run

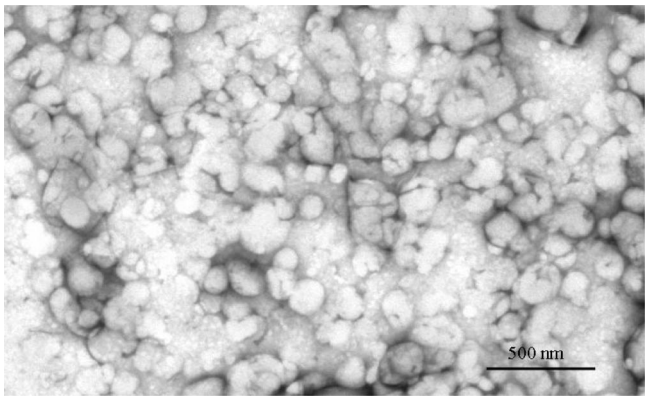

Figure 5. TEM micrographs of the negative stained nanocomposite latex MPCO.

MPCO was different than that for runs MP and MPCM. The polymerization temperature was 90 °C in that case and the redox initiator couple was only added after 4 h of polymerization. During the stage without initiator addition the conversion reached 21.5%, indicating that polymerization started in the interlayer space of the clay due to presence of the macroinitiator (see Figure 3: the first point of the conversion vs time curve for run MPCO). It is worth noting that after adding the redox initiators, the polymerization evolved at a lower polymerization rate for the SG1 containing clay even though it was polymerized at higher temperature. It can also be noticed that the polymerization for run MPCM was very fast, and full conversion was achieved in 30 min. All the nanocomposite latexes were stable and presented no coagulum, indicating that all the modified clay added in the formulation had been incorporated in the final latex.

Table 3 lists the monomer miniemulsion droplet size and final particle size of the latexes MP, MPCO and MPCM measured by light scattering.

Light scattering measurements showed that the droplet size of miniemulsion containing clay was larger than the counterpart without modified clay, probably due to the presence of the clay on the droplet surface. The final particle sizes were smaller than those of the initial miniemulsion droplet, indicating that some particles were produced through mechanisms other than droplet nucleation.

Using a parking area of 131Å^2/molecule[56] for SLS on MMA/BA copolymer, the surface area that could be covered by the emulsifier was calculated for runs MP, MPCO and MPCM. Table 4 lists the total droplets surface area (A_D), the surface area that could be covered by the emulsifier (A_E, assuming 100% coverage), the free available emulsifier concentration and the ratio of the number of polymer particles times the number of initial droplets, N_p/N_d, for runs MP, MPCO, and MPCM. It can be observed that the available surface area to be covered by the emulsifier was higher than the surface area formed by the miniemulsion droplets for all the cases. Taking into account

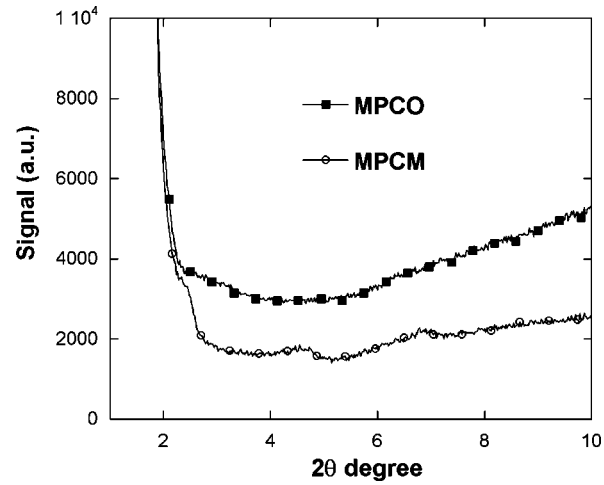

Figure 7. WAXD patterns of nanocomposite latex films MPCO and MPCM.

that the CMC of SLS is 8 mM,[57] it can be concluded that micelles were presented in the medium. The polymer particle number/droplet number ratios (N_p/N_d) of these runs were higher than 1, indicating that new particles were generated during the polymerization, likely due to the presence of micelles in the medium. Therefore, it is likely that micellar nucleation occurred during these polymerizations.

Characterization of the Waterborne Nanocomposites. First of all the morphology of the waterborne poly (methyl methacrylate-*co*-butyl acrylate)/hydrophobized reactive clay nanocomposite latexes and films is discussed. Then, the microstructural characterization of the nanocomposites is performed in terms of MWD and characterization of the polymer produced inside and outside the clay layers. Finally, the mechanical, thermal and barrier properties of the nanocomposites are presented and compared with those of the pristine miniemulsion latex prepared under the same conditions (without clay).

Morphology of the Waterborne Nanocomposites. The morphology of the nanocomposite latexes was analyzed by both SAXS and TEM techniques. On the other hand, the morphology of the dried films obtained from the latexes was analyzed by WAXD technique. Additional to XRD techniques, the dried films were also analyzed by TEM to confirm the structure of the clay in the polymer matrix.

In order to shed some light on the location of the clay platelets in the final nanocomposite latexes, SAXS measurements of the liquid latexes were performed. The SAXS patterns of the blank latex, MP and the nanocomposite latexes containing reactive montmorillonite clays, MPCO and MPCM are presented in Figure 4. The scattering intensity of the blank latex, MP, shows the presence of the typical fringes arising from the scattering of the spherical particles.[58] However these fringes appeared

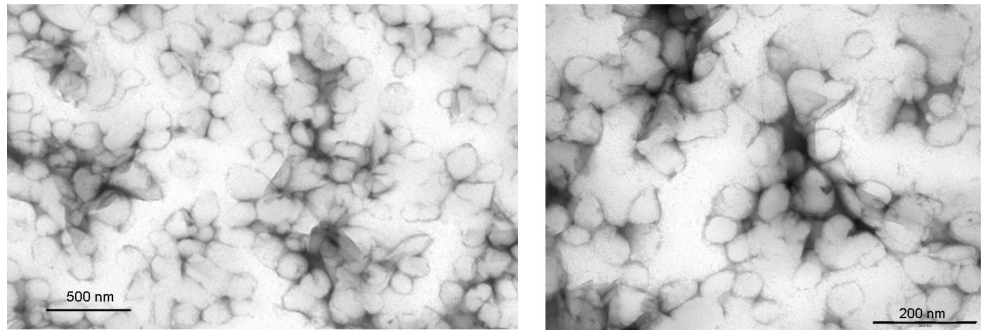

Figure 6. TEM micrographs of the negative stained nanocomposite latex MPCM.

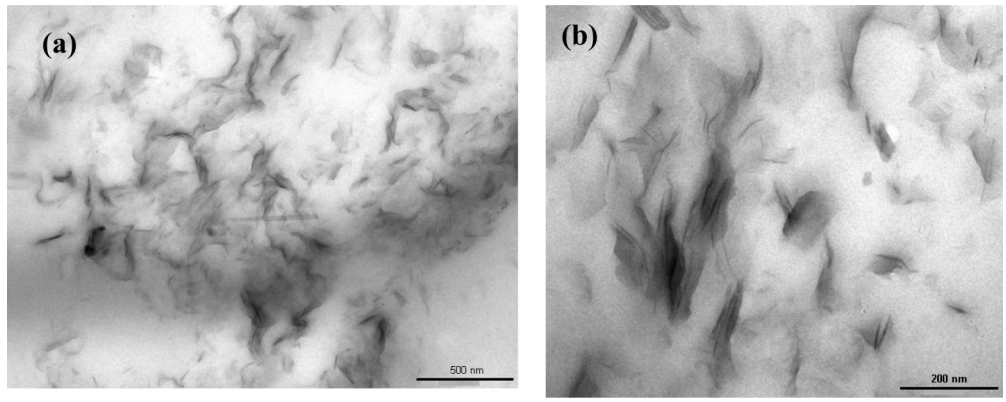

Figure 8. TEM micrographs of nanocomposite latex MPCO film at different magnifications.

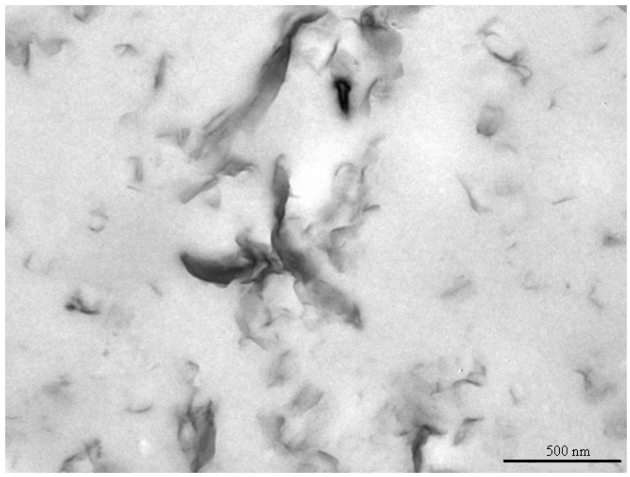

Figure 9. TEM micrographs of nanocomposite latex MPCM film.

Table 5. The Sol M_w, the Polydispersity Index, and the Gel Content for Runs MP, MPCO, and MPCM

run	M_w (g/mol)	PDI (M_w/M_n)	gel content (%)[a]
MP	6.3×10^5	6.1	5.0
MPCO	1.7×10^5	2.7	13.6
MPCM	9.9×10^4	2.5	15.2

[a] The clay, which is also insoluble, is already subtracted in the given value.

attenuated in the spectra of MPCO and MPCM latexes, which were attributed to the presence of clay platelets on their surface. Therefore and due to the hydrophobic character of the reactive montmorillonite clays, a preferential polymer particle surface location of the clay platelets can be suggested (as in the pickering emulsions[59,60]).

Figures 5 and 6 show the TEM micrographs of the negatively stained MPCO and MPCM latexes.

Unfortunately, the clay platelets cannot be clearly distinguished in the images. In the case of waterborne nanocomposite MPCO, irregular nonspherical particle shapes can be seen in the micrographs which might be a consequence of the clay presence. In the case of waterborne nanocomposite MPCM, much sharper particle limits were observed and may indicate the presence of the clay on the particle surface.

The morphology of the waterborne nanocomposite films was mainly studied by means of WAXD and TEM techniques. Figure 7 shows the WAXD patterns of the nanocomposites latex films MPCO and MPCM synthesized by batch miniemulsion polymerization. It can be observed that no diffraction peaks appeared in none of the WAXD patterns of the nanocomposites

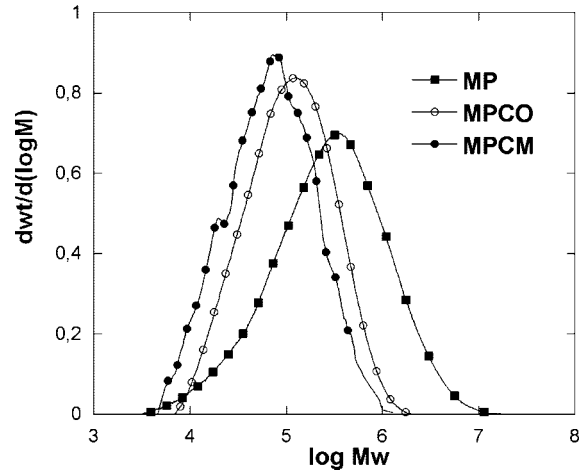

Figure 10. Molecular weight distribution for runs MP, MPCO, and MPCM.

Table 6. M_w of the Polymer Formed Outside and Inside of the Clay Platelets for Runs MPCO and MPCM

	M_w (g/mol)	
run	inside polymer	outside polymer
MPCO	576	1.7×10^5
MPCM	648	7.9×10^4

(apart from those characteristic SLS peaks for run MPCM), indicating that the basal spacing of the hydrophobized reactive clays were extended beyond the separation of clay platelets and nanocomposites with exfoliated structures and an average basal distance higher than 4 nm were obtained.

Figures 8 and 9 present the TEM micrographs of the nanocomposite latex films of MPCO and MPCM at different magnifications. Upon the nanocomposite film formation, the hydrophobized reactive clays were well dispersed in the polymer matrix and individual layers as well as zones with more than one clay layer can be distinguished. These micrographs are in agreement with the WAXD patterns presented in Figure 7.

Molecular Weight Distribution. Table 5 presents the weight average molecular weight, polydispersity index, and gel contents for latexes MP, MPCO, and MPCM.

It can be observed that nanocomposite latexes presented higher gel polymer content than the blank latex, MP. The reason for the high gel polymer formation for latex MPCO should be attributed to the higher reaction temperature (90 °C) that enhanced H abstraction in the polymer backbone even though monomer conversion was lower during the polymerization. The polymerization for latex MPCM was carried out at 70 °C, like the blank MP, but the gel content was higher likely because

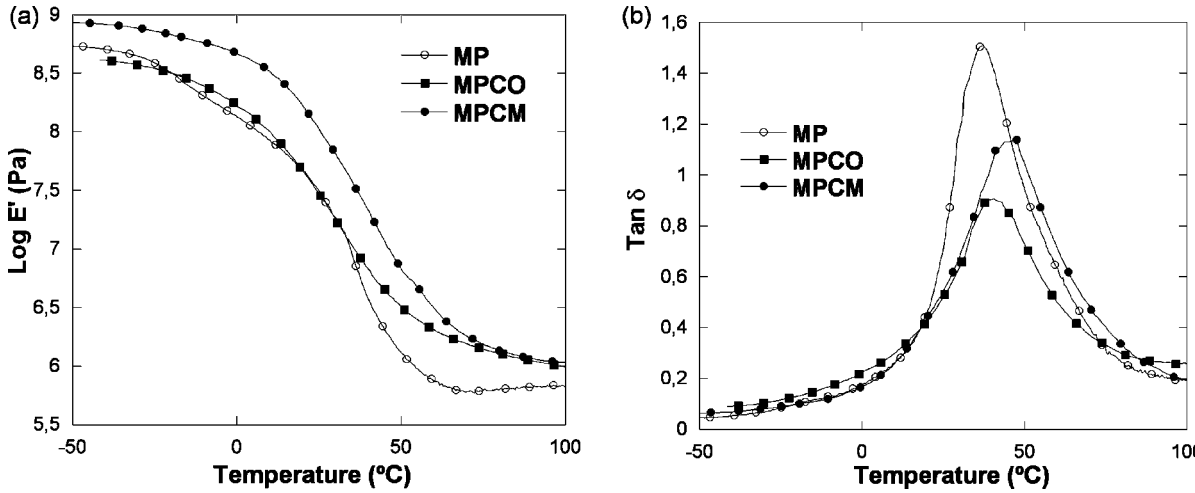

Figure 11. DMTA traces of the pure copolymer and nanocomposite latex films MPCO and MPCM: (a) temperature dependence of storage modulus, and (b) temperature dependence of tan δ.

Table 7. Thermal Stability, Water Vapor Permeability, and Contact Angle Data for Runs MP, MPCO, and MPCM

run	decomposition temperature, $T_{d\ max}$[a] (°C)	char (%) real	char (%) theoretical	WVTR (g mm/cm^2 days) As prepared	WVTR (g mm/cm^2 days) Rinsed film	contact angle As prepared	contact angle Rinsed film
MP	387	1.3		24.6 ± 0.9	19.0 ± 1.5	66.5	69.4
MPCO	417	4.3[b]	4	19.2 ±0.2	16.4 ± 0.5	65.4	74.2
MPCM	419	2.7[b]	1.8	17.4 ± 0.2	15.7 ± 0.7	64.4	71.0

[a] Calculated from the maximum derivative weight loss versus temperature curve, [b] Calculated extracting the char that corresponds to pure copolymer (1.3%).

full conversion was achieved faster than for MP and H abstraction events lasted longer producing more gel.

The soluble polymer fraction obtained after Soxhlet extraction was analyzed by size exclusion chromatography. The sol MWDs are presented in Figure 10. The sol molecular weight and MWD are in agreement with the gel polymer contents. The higher the gel content the lower the molecular weight of the soluble polymer fractions because of the preferential incorporation of the long chains to the gel fraction.

Table 6 lists the average molecular weight of the polymer formed inside (obtained by reverse cationic exchange) and outside of the clay platelets for runs MPCO and MPCM.

First of all and as was expected, the M_w of the outside polymer was very similar to the one obtained by Soxhlet extraction. However, the very small molecular weights of the inside "polymer" were not expected at all. In case of latex MPCO, the M_w was even smaller than that of the macroinitiator used to modify the clay (1170 g/mol). In the case of MPCM, the M_w is only slightly higher than the MA16 unit (462 g/mol). In order to understand these unexpected results, ^{1}H NMR spectra of the polymers were carried out.

In the ^{1}H NMR spectra (see Supporting Information) of the outside polymer extracted from nanocomposite MPCO the presence of the cationic macroinitiator could be identified. Due to the high pH used in the miniemulsion polymerizations (pH = 9), the quaternary ammonium groups of the cationic oligomer could be converted into an amidine group. This might favor the detachment of the modifier from the interlayer space of the clay layer. On the other hand, in the first extraction step with THF the polymer attached to the clay platelets might have been extracted, which would also explain the presence of the macroinitiator in the outside polymer and the low molecular weight of the inside "polymer" extracted from the clay layer. Xu et al.[61] in the synthesis of poly (styrene-*co*-methyl methacrylate)/clay nanocomposites with a reactive surfactant (AMPS, 2-acrylamido-2-methyl-1-propanesulfonic acid) by emulsion polymerization in the presence of 3 and 5 wt % pristine Na−MMT also found that the molecular weight of the molecules tethered on the silicates after reverse cationic exchange were lower by 3 orders of magnitude than the average molecular weight of the poly(S-*co*-MMA) obtained by the extraction of the nanocomposite with THF.

For run MPCM it is worth pointing out that filtered MA16-MMT clay was employed in the miniemulsion polymerization process. The ^{1}H NMR spectra of the inside and outside polymers (see Supporting Information) did not present any methine (CH_2=C−) protons of MA16 which is an indication that MA16 monomer had polymerized. The fact that filtered MA16-MMT was used explains that nonattached MA16 containing polymer chains were extracted from the nanocomposite, but an explanation for the low molecular weight of the polymer attached to the clay layer cannot be offered.

The End-Use Properties of Waterborne Acrylic/Reactive Montmorillonite Nanocomposites. The end-use mechanical, thermal and barrier properties of the waterborne acrylic polymer/reactive montmorillonite clay nanocomposites were investigated and compared to the pristine copolymer.

a. Mechanical Properties. The dynamic mechanical properties (DMTA) of the nanocomposites were measured and compared to those of the pristine copolymer. Figure 11 shows the DMTA traces: temperature dependence of log E' and tan δ for runs MP, MPCO−MPCM.

It can be seen that at temperatures above T_g (≈40 °C) the storage modulus for both nanocomposites is higher than that of the pure copolymer. This enhancement was more pronounced in the solid state region of the material in the case of MPCM. It indicates that stress transfer from matrix to the reinforcer was more effective in the case of organomodifier with shorter chain length. Since the covalent bonding was not proved in this case, the hydrogen bonding between acrylate group of MA16 and polymer backbone was enough to facilitate this interfacial stress transfer. Since the stress transfer is controlled by the matrix shear stress at the interface,[62] the longer chain of the oligomeric

organomodifier probably causes the decrease of this shear, what leads to a lower reinforcement effect.

The glass transition temperature of the nanocomposites MPCO and MPCM was increased by 3.6 and 8.3° respectively compared to the counterpart without clay, MP. Previous conclusions can be applied again; MA16 more effectively constraints the cooperational motion of polymeric backbone segments and thus the T_g is shifted to higher temperatures. On the other hand the oligomeric structure of the living cationic oligomer facilitates the segmental motions at lower temperatures than in the case of MA16, but probably thanks to covalent bonding not in such extent as can be seen from the smaller loss factor.

b. Thermal Properties. The thermal stability of the nanocomposites was investigated by measuring the temperature dependence of weight loss through thermo-gravimetric analysis. The TGA data for runs MP, MPCO and MPCM (see Supporting Information) are presented in Table 7 including the maximum decomposition temperature, $T_{d,max}$ calculated from the maximum of the derivative weight loss versus temperature curve, and the amount of material not volatile at 600 °C.

An improvement in the thermal stability of the nanocomposites was found compared to the pure copolymer. An increase between 30 and 32 °C in the decomposition temperature was obtained for both nanocomposites compared to the counterpart without clay. The increase of the decomposition temperature is likely due to the clay that acts as a heat barrier. It can be noticed that the amount of the recovered clay was slightly higher than the loaded amount for both nanocomposites, which can be attributed to the heterogeneous distribution of the clay during film formation.

c. Barrier Properties. The water vapor permeability was studied by measuring water vapor transmission rate, WVTR, for the nanocomposite films and for the pristine copolymer film. Table 7 lists the WVTR and contact angle data for as-prepared and rinsed films of the pure copolymer, MP and nanocomposites MPCO and MPCM (measurements were carried out on the film-air interface). It can be noticed that the WVTR decreased for all the nanocomposites as-prepared films compared to the pure copolymer, likely due to the tortuous diffusion path that retards the progress of the water molecule through the polymer film.[63] In all the cases the WVTR decreased when the latex film was rinsed with distilled water because we got rid of the fraction of SLS that migrated to the surface during the film formation.[64] This is in agreement with the contact angle data of the film-air interface (see Table 7) that showed the film-air interface to be more hydrophilic without rinsing the film. Aramendia et al.[64] have found that mass transfer was faster the more hydrophilic was the interface.

Conclusions

Montmorillonite clay was successfully exchanged with a cationic macromonomer (MA16) and a cationic macroinitiator (acrylic oligomer end-capped with a nitroxide group) synthesized in this work. The direct use of these hydrophobized reactive montmorillonite clays in miniemulsion polymerization process allowed the production of stable and coagulum free 30% solids content waterborne acrylic polymer/clay nanocomposites with partially exfoliated structures as proved by X-ray diffraction and TEM techniques. These waterborne nanocomposites exhibited improved mechanical, thermal and barrier properties compared to pristine copolymer prepared under the same conditions but without clay. However, the end-tethering of the acrylic polymer to the clay could not be proved. Unexpected small molecular weight polymer chains attached to the clay were extracted from the clay interlayer of the nanocomposites. This made us believe that either during the miniemulsion preparation at basic pH the organic cationic modifier could have left the clay interlayer space or that during the initial step of polymer recovery the polymer chains formed within the clay interlayer space were extracted in the case of the cationic macroinitiator, and that polymerization in the interlayer space proceeded only to a very limited extent in the case of MA16 modified montmorillonite.

Acknowledgment. G.D. acknowledges the fellowship by the Marie Curie program (HPMT-CT-2001-00227). The support by the Ministerio de Educación y Ciencia of Spain (MAT 2003-01963, CTQ 2006-03412/PPQ), European Union (Napoleon project IP 011844-2), and Gobierno Vasco (Nanomateriales, ETORTEK2005) is gratefully acknowledged. The authors want to thank to Dr. Francois Fauth and Dr. Ana Labrador for the SAXS measurements at the Spanish CRG beamline at the European Synchrotron Radiation Facility in Grenoble.

Supporting Information Available: Figures showing ^{1}H NMR spectra and TGA curves and a discussion of these results. This material is available free of charge via the Internet at http://pubs.acs.org.

References and Notes

(1) Ploehn, H. J.; Liu, Ch. *Ind. Eng. Chem. Res.* **2006**, *45*, 7025.
(2) Paul, D. R.; Robeson, L. M. *Polymer* **2008**, *49*, 3187.
(3) Yano, K.; Usuki, A.; A.; Okada, A. *J. Polym. Sci., Part A: Polym. Chem.* **1997**, *35*, 2289.
(4) Koo, C. M.; S.K.; Kim, S. K.; Chung, I. J. *Macromolecules* **2003**, *36*, 2748.
(5) Sinha Ray, S.; Okamoto, K.; Okamoto, M. *Macromolecules* **2003**, *36*, 2355.
(6) Usuki, A.; Kojima, Y.; Okada, A.; Fukushima, Y.; Kurauchi, T.; Kamigaito, O. *J. Mater. Res.* **1993**, *8*, 1174.
(7) Liu, L.; Qi, Z.; Zhu, X. *J. Appl. Polym. Sci.* **1999**, *71*, 1133.
(8) Li, Y.; Zhao, B.; Xie, S.; Zhang, S. *Polym. Int.* **2003**, *52*, 892.
(9) Fu, X.; Qutubuddin, S. *Polymer* **2001**, *42*, 807.
(10) Kawasumi, M.; Hasegawa, N.; Musuki, A.; Okada, A. *Macromolecules* **1997**, *30*, 6333.
(11) Lan, T.; Pinnavaia, T. J. *Chem. Mater.* **1994**, *6*, 2216.
(12) Massersmith, P. B.; Giannelis, E. P. *J. Polym. Sci., Part A: Polym. Chem.* **1995**, *33*, 1047.
(13) Fornes, T. D.; Hunter, D. L.; Paul, D. R. *Macromolecules* **2004**, *37*, 1793.
(14) Pospisil, M.; Capkova, P.; Merinska, D.; Malac, Z.; Simonik, J. *J. Colloid Interface Sci.* **2001**, *236*, 127.
(15) Wang, D.; Zhu, J.; Yao, Q.; Wilkie, C. A. *Chem. Mater.* **2002**, *14*, 3837.
(16) Gilman, J. W.; Awad, W. H.; Davis, R. D.; Shields, J.; Harris, R. H.; Davis, C.; Morgan, A. B.; Sutto, T. E.; Callahan, J.; Trulove, P. C.; DeLong, H. C. *Chem. Mater.* **2002**, *14*, 3776.
(17) Yeh, J. M.; Liou, S. J.; Lai, M. C.; Chang, Y. W.; Huang, C. Y.; Chen, C. P.; Jaw, J. H.; Tsai, T. Y.; Yu, Y. H. *J. Appl. Polym. Sci.* **2004**, *94*, 1936.
(18) Okamoto, M.; Morita, S.; Taguchi, H.; Kim, Y. H.; Kotaka, T.; Tateyama, H. *Polymer* **2000**, *41*, 3887.
(19) Huang, X.; Brittain, W. J. *Macromolecules* **2001**, *34*, 3255.
(20) Fan, X.; Xia, C.; Advicula, R. C. *Colloid Surf. A: Phys. Eng. Asp.* **2003**, *219*, 75.
(21) Zeng, C.; Lee, L. J. *Macromolecules* **2001**, *34*, 4098.
(22) Su, S.; Jiang, D.; Lee, Y. S. *Colloids Surf. A* **2004**, *15*, 225.
(23) Akelah, A.; Moet, A. *J. Mater. Sci.* **1996**, *31*, 3589.
(24) Fan, X.; Xia, C.; Advincula, R. C. *Langmuir* **2005**, *21*, 2537.
(25) Weimer, M. W.; Chen, H.; Giannelis, E. P.; Sogah, D. Y. *J. Am. Chem. Soc.* **1999**, *121*, 1615.
(26) Di, J.; Sogah, D. Y. *Macromolecules* **2006**, *39*, 1020.
(27) Konn, C.; Morel, F.; Beyou, E.; Chaumont, P.; Bourgeat-Lami, E. *Macromolecules* **2007**, *40*, 7464.
(28) Zhang, B. Q.; Pan, C. Y.; Hong, C. Y.; Luan, B.; Shi, P. J. *Macrom. Rapid Commun.* **2006**, *27*, 92.
(29) Chiefari, J.; Chong, Y. K.; Ercole, F.; Krstina, J.; Jeffery, J.; Le, T. P. T.; Mayadunne, R. T. A.; Meijs, G. F.; Moad, C. L.; Moad, G.; Rizzardo, E.; Thang, S. H. *Macromolecules* **1998**, *31*, 5559.
(30) Lee, D. C.; Jang, L. W. *J. Appl. Polym. Sci.* **1996**, *61*, 1117.
(31) Choi, Y. S.; Choi, M. H.; Wang, K. H.; Kim, S. O.; Kim, Y. K.; Chung, I. J. *Macromolecules* **2001**, *34*, 8978.
(32) Diaconu, G.; Paulis, M.; Leiza, J. R. *Ploymer* **2008**, *49* (10), 2444.

(33) Bandyopadhyay, S.; Hsieh, A. J.; Giannelis, E. P. *ACS Symp. Ser.* **2002**, *84*, 15.
(34) Li, H.; Yang, Y.; Yu, Y. Z. *J. Adhes. Sci. Technol.* **2004**, *18*, 1759.
(35) Park, B. J.; Kim, T. H.; Choi, H. J.; Lee, J. H. *J. Macromol. Sci., Part B: Phys.* **2007**, *46*, 341.
(36) Negrete-Herrera, N.; Putaux, J. L.; David, L.; Bourgeat-Lami, E. *Macromolecules* **2006**, *39*, 9177.
(37) Herrera, N. N.; Persoz, S.; Putaux, J. L.; David, L.; Bourgeat-Lami, E. *J. Nanosci. Nanotechnol.* **2006**, *6*, 42.
(38) Li, H.; Yu, Y. Z.; Yang, Y. K. *Eur. Polym. J.* **2005**, *41*, 2016.
(39) Min, H. L.; Wang, J. H.; Hui, H.; Jie, W. *J. Macromol. Sci., Part B: Phys.* **2006**, *45*, 623.
(40) Park, B. J.; Choi, H. J. *Sci. Technol. Hybrid Mater.* **2006**, *111*, 187.
(41) Wang, T.; Wang, M. Z.; Zhang, Z. C.; Ge, X. W.; Fang, Y. E. *Mater. Lett.* **2006**, *60*, 2544.
(42) Ugelstad, J.; El-Aasser, M. S.; Vaderhoff, J. W. *J. Polym. Sci. Lett.* **1973**, *11*, 503.
(43) Asua, J. M. *Prog. Polym. Sci.* **2002**, *27*, 1283.
(44) Sun, Q. H.; Deng, Y. L.; Wang, Z. L. *Macromol. Mater. Eng.* **2004**, *289*, 288.
(45) Tong, Z.; Deng, Y. *Ind. Eng. Chem. Res.* **2006**, *45*, 2641.
(46) Moraes, R. P.; Santos, A. M.; Oliveira, P. C.; Souza, F. C. T.; do Amaral, M.; Valera, T. S.; Demarquette, N. R. *Macromol. Symp.* **2006**, *245/246*, 106.
(47) Lorah, D. P.; Slone R. V.; Madle T. G. WO/0224756, **2002**.
(48) Diaconu, G.; Paulis, M.; Leiza, J. R. *Macrom. React. Eng.* **2008**, *2*, 80.
(49) Zeng, C.; Lee, L. J. *Macromolecules* **2001**, *34*, 4098.
(50) Salem, N.; Shipp, D. A. *Polymer* **2005**, *46*, 8573.
(51) Charleux, B.; Nicolas, J.; Guerret, O. *Macromolecules* **2005**, *38*, 5485.
(52) Tombácz, E.; Szekeres, M. *Appl. Clay Sci.* **2004**, *24*, 75.
(53) Elizalde, O.; Leiza, J. R.; Asua, J. M. *Ind. Eng. Chem. Res.* **2004**, *43*, 7401.
(54) Miguel, O.; Fernandez-Berridi, M. J.; Iruin, J. J. *J. Appl. Polym. Sci.* **1997**, *64*, 1849.
(55) Marras, S. I.; Tsimpliaraki, A.; Zuburtikudis, I.; Panayiotou, C. *J. Colloid Interface Sci.* **2007**, *315*, 520.
(56) Rosen, M. J., *Surfactants and interfacial phenomena*, 3rd ed.; John Willey & Sons: New York, 1989.
(57) Van Os, N. M.; Haak, J. R.; Rupert, L. A. M., *Physico-Chemical Properties of the Selected Anionic, Cationic and Nonionic Surfactants*; Elsevier: Amsterdam, 1993.
(58) Svergun, D. I.; Koch, M. H. J. *Rep. Prog. Phys.* **2003**, *66*, 1735.
(59) Liesegang, R. E. *Kolloid-Z.* **1928**, *45*, 370.
(60) Cauvin, S.; Colver, P. J.; Bon, S. A. F. *Macromolecules* **2005**, *38*, 7887.
(61) Xu, M.; Choi, Y. S.; Kim, Y. K.; Wang, K. H.; Chung, I. J. *Polymer* **2003**, *44*, 6387.
(62) Coleman, J. N.; Khan, U.; Blau, W. J.; Gun'ko, Y. K. *Carbon* **2006**, *44*, 1624.
(63) Okamoto, M. *Encycl. Nanosci. Nanotechnol.* **2004**, *8*, 791.
(64) Aramendia, E.; Barandiaran, M. J.; Grade, J.; Asua, J. M. *Langmuir* **2005**, *21*, 1428.

MA802467J